

Electronic Supplementary Information

Hierarchically porous Fe/N-C hollow spheres derived from melamine/Fe-incorporated polydopamine for efficient oxygen reduction reaction electrocatalysis

Bomin Feng,^{ab} Xiuju Wu,^a Yanli Niu,^a Wei Li,^a Yunxi Yao,^{*b} Weihua Hu^{*a} and Chang Ming Li^a

^a Institute for Clean Energy & Advanced Materials, School of Materials & Energy,
Southwest University, Chongqing, China and Chongqing Key Laboratory for
Advanced Materials and Technologies of Clean Energies, Chongqing 400715, China.

E-mail: whhu@swu.edu.cn (W. H. Hu)

^b Institute of Materials, China Academy of Engineering Physics, Mianyang 621908,
China. E-mail: yaoyunxi2017@163.com (Y. X. Yao)

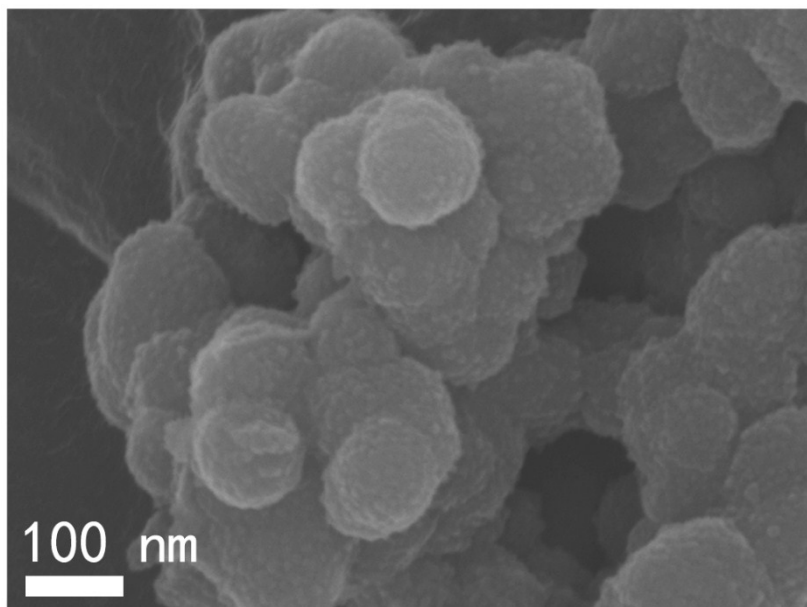


Fig. S1 SEM image of PDA-Fe-melamine precursor.

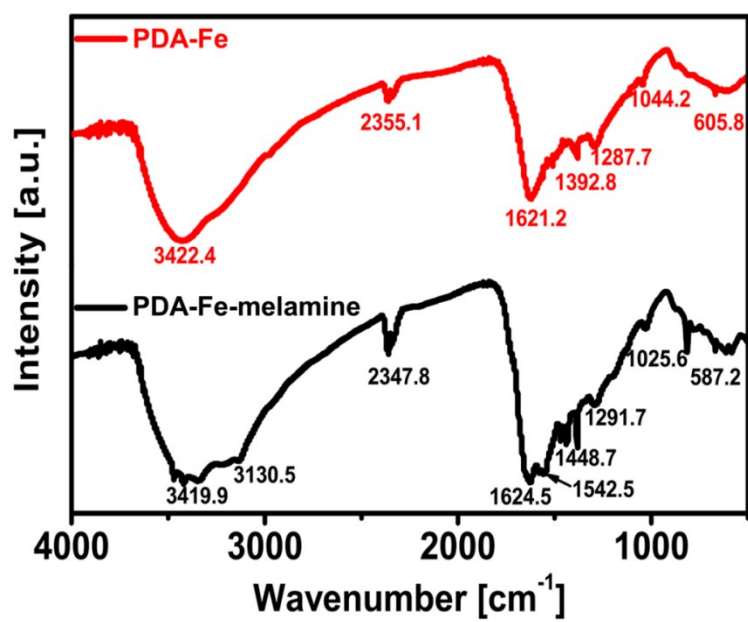


Fig. S2 FTIR spectra of PDA-Fe-melamine precursor and PDA-Fe precursor.

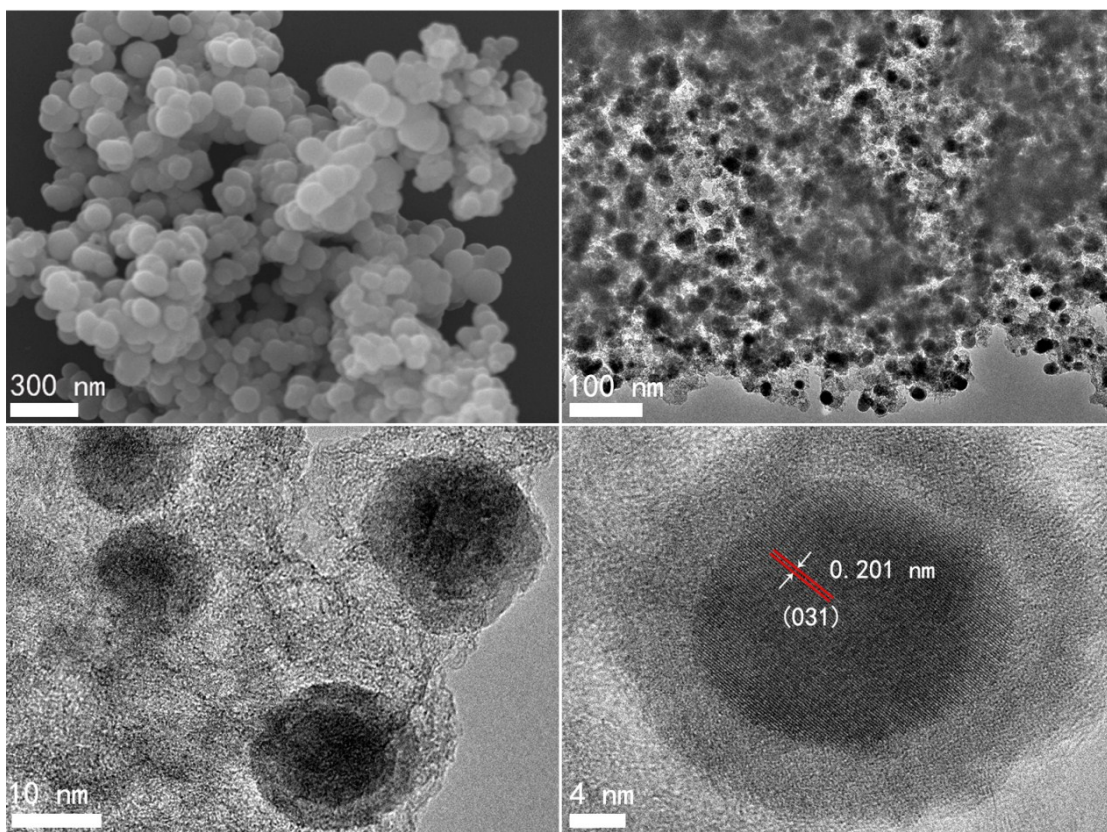


Fig. S3 FESEM and TEM images of $\text{Fe}_3\text{C}@\text{N-C}$ catalyst synthesized by pyrolysis of PDA-Fe precursor.

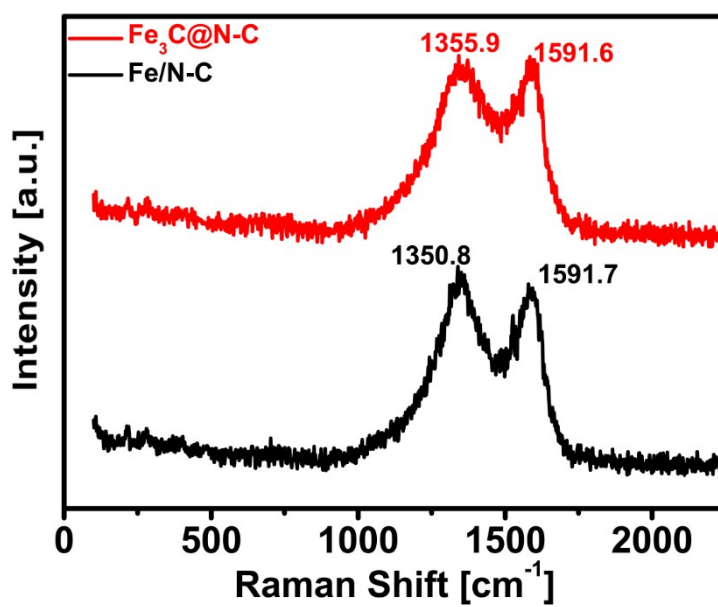


Fig. S4 Raman spectra of Fe/N-C and $\text{Fe}_3\text{C}@\text{N-C}$ catalyst.

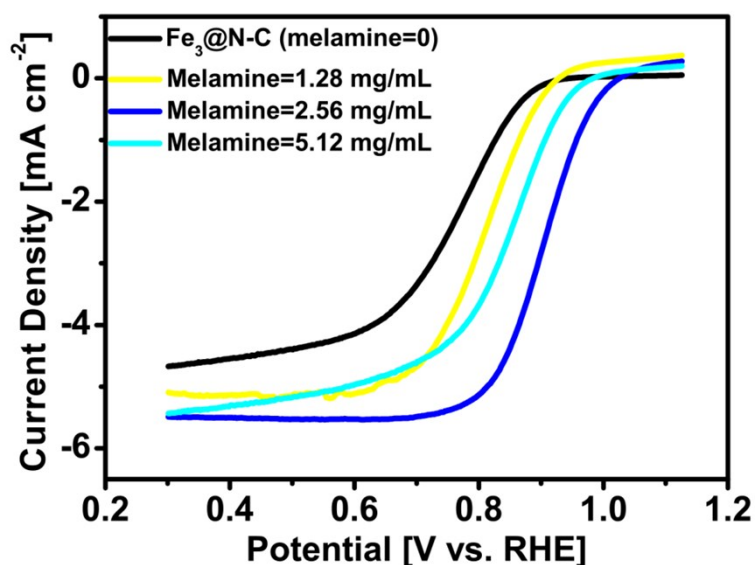


Fig. S5 Optimizing alkaline ORR activity of Fe/N-C catalysts by changing the dosage of melamine. LSV curves of a batch of Fe/N-C catalysts synthesized with different concentration of melamine at 0, 1.28, 2.56 and 5.12 mg mL⁻¹, respectively. (Other parameters remain constant including DA=1.28 mg mL⁻¹, Fe concentration=1 mM, pyrolysis at 800 °C. LSV curves measured in O₂-saturated 0.1 M KOH, scan rate: 10 mV s⁻¹, rotation rate: 1600 rpm).

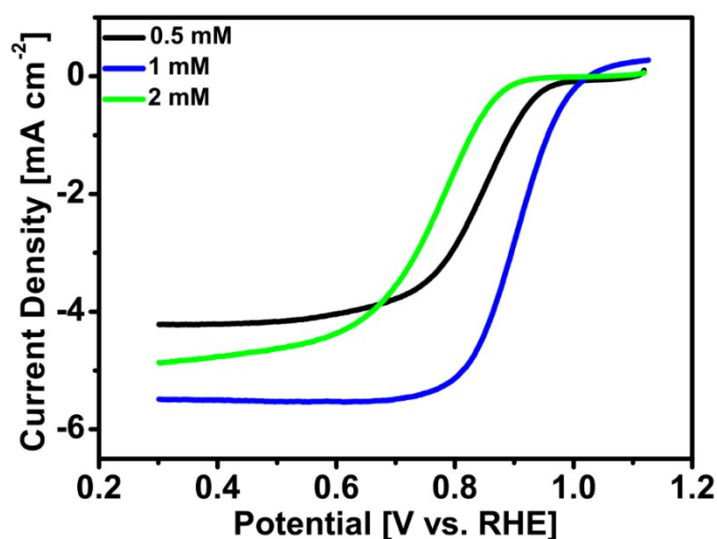


Fig. S6 Optimizing alkaline ORR activity of Fe/N-C catalysts by changing the dosage of Fe³⁺ concentration from 0.5 to 2.0 mM. (Other parameters remain constant including DA=1.28 mg mL⁻¹, melamine concentration=2.56 mg mL⁻¹, pyrolysis at 800 °C. LSV curves measured in O₂-saturated 0.1 M KOH, scan rate: 10 mV s⁻¹, rotation rate: 1600 rpm).

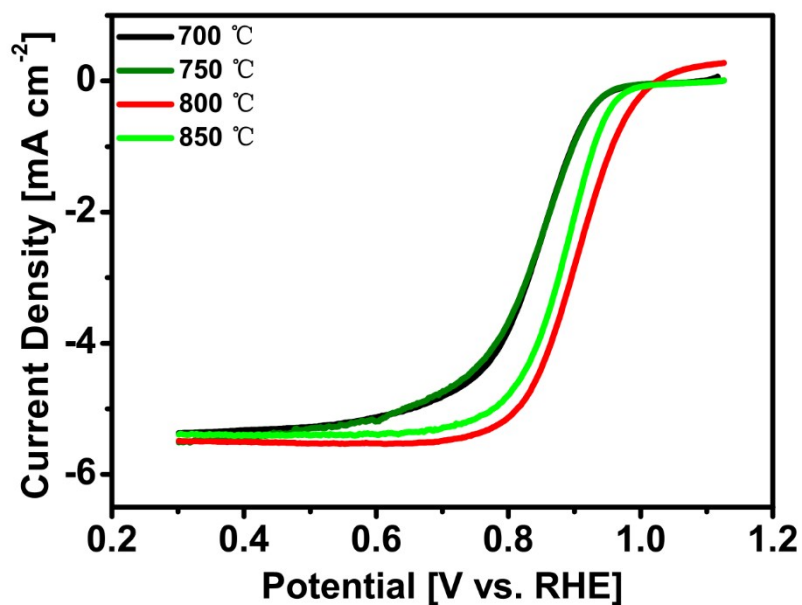


Fig. S7 Optimizing alkaline ORR activity of Fe/N-C catalysts by changing the pyrolysis temperature. (Other parameters remain constant including DA=1.28 mg mL⁻¹, melamine concentration=2.56 mg mL⁻¹, Fe³⁺ concentration 1.0 mM. LSV curves measured in O₂-saturated 0.1 M KOH, scan rate: 10 mV s⁻¹, rotation rate: 1600 rpm).

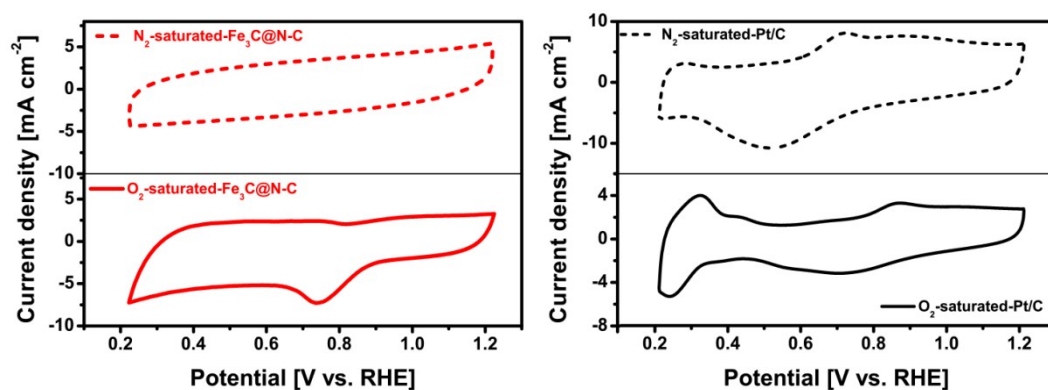


Fig. S8 CV curves of Fe₃C/N-C catalyst and Pt/C catalyst measured in O₂-saturated and N₂-saturated 0.1 M KOH, scan rate: 100 mV s⁻¹.

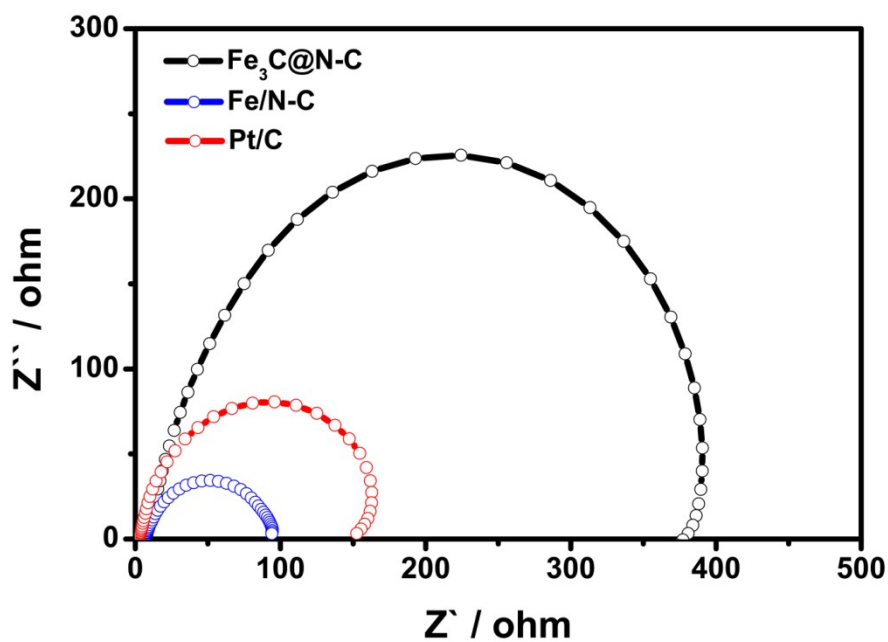


Fig. S9 EIS curves of Fe/N-C, Fe₃C/N-C and Pt/C catalysts measured in O₂-saturated 0.1 M KOH. (Applied potential: 0.95 V vs. RHE, amplitude of AC signal perturbation: 5 mV, frequency range: 100 kHz to 10 mHz).

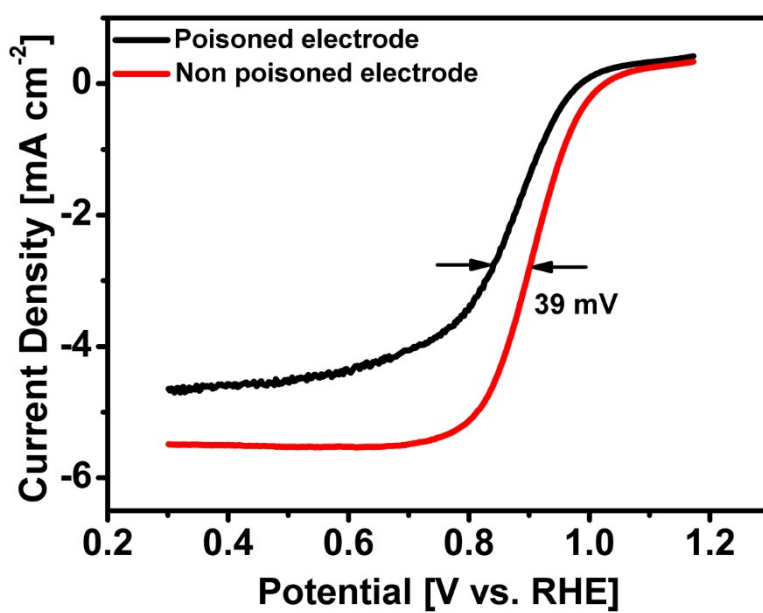


Fig. S10 Alkaline ORR activity of Fe/N-C catalysts before and after immersing in 10 mM KSCN for 1 h. (Electrolytes: O₂-saturated 0.1 M KOH, scan rate: 10 mV s⁻¹, rotation rate: 1600 rpm).

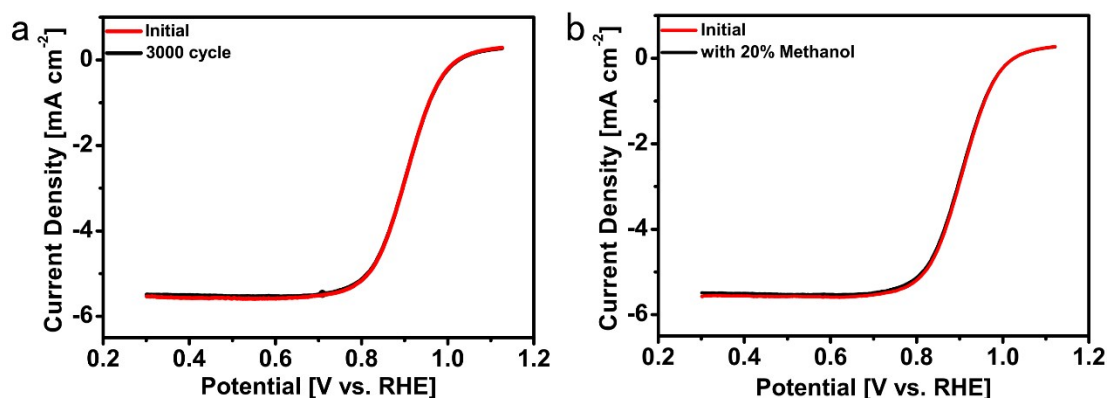


Fig. S11 (a) LSV curves of Fe/N-C before and after 3000-cycle ADT. (b) LSV curves with and without 20 % methanol (v/v). (Electrolytes: O₂-saturated 0.1 M KOH, scan rate: 10 mV s⁻¹, rotation rate: 1600 rpm).

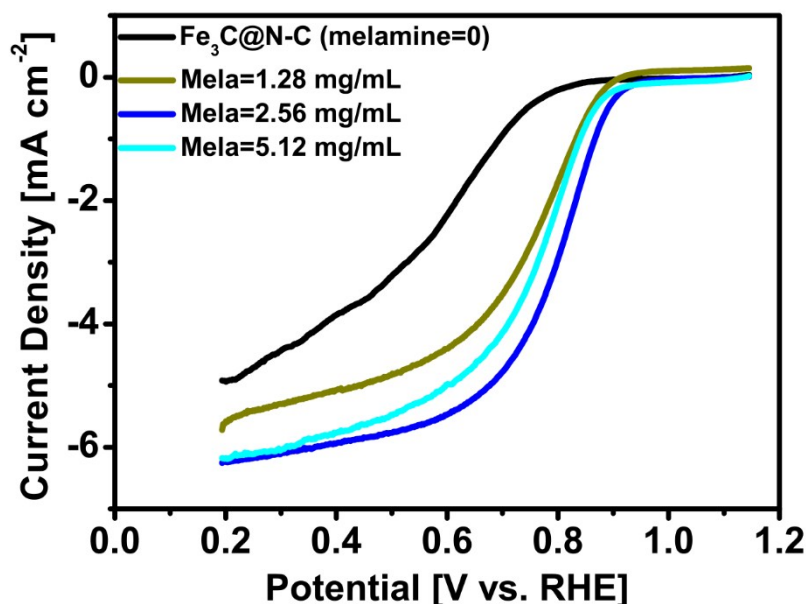


Fig. S12 Optimizing acidic ORR activity of Fe/N-C catalysts by changing the dosage of melamine. LSV curves of a batch of Fe/N-C catalysts synthesized with different concentration of melamine at 0, 1.28, 2.56 and 5.12 mg mL⁻¹, respectively. (Other parameters remain constant including DA=1.28 mg mL⁻¹, Fe concentration=1 mM, pyrolysis at 800 °C. LSV curves measured in O₂-saturated 0.1 M HClO₄, scan rate: 10 mV s⁻¹, rotation rate: 1600 rpm).

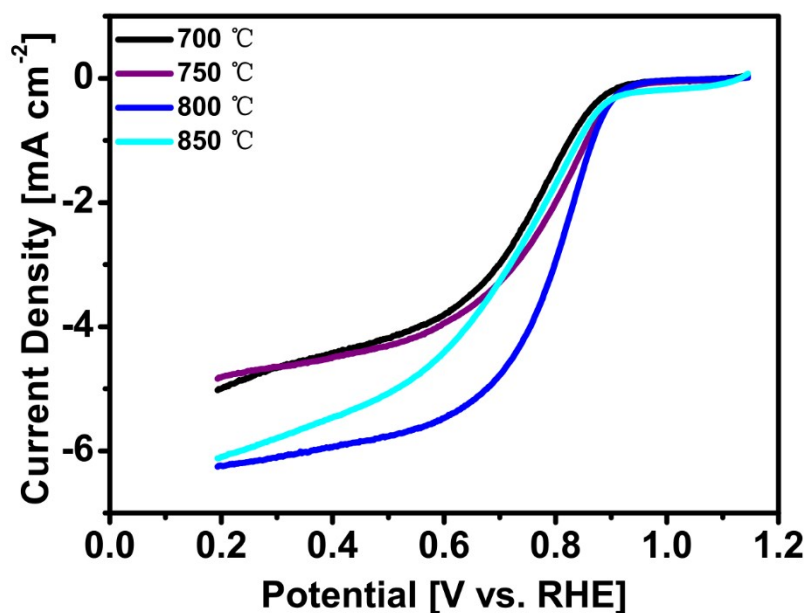


Fig. S13 Optimizing acidic ORR activity of Fe/N-C catalysts by changing the pyrolysis temperature. (Other parameters remain constant including DA=1.28 mg mL⁻¹, melamine concentration=2.56 mg mL⁻¹, Fe³⁺ concentration 1.0 mM. LSV curves measured in O₂-saturated 0.1 M HClO₄, scan rate: 10 mV s⁻¹, rotation rate: 1600 rpm). (Electrolytes: O₂-saturated 0.1 M HClO₄, scan rate: 10 mV s⁻¹, rotation rate: 1600 rpm).

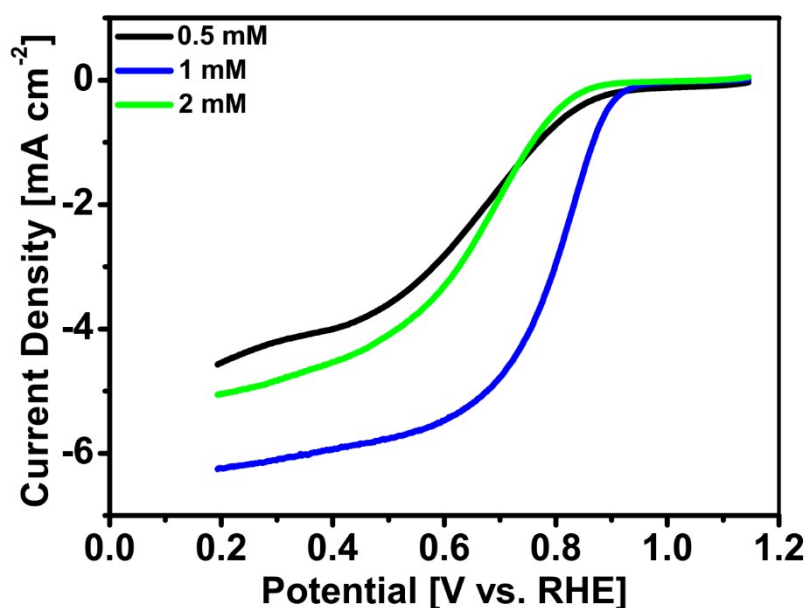


Fig. S14 Optimizing acid ORR activity of Fe/N-C catalysts by changing the dosage of Fe³⁺ concentration from 0.5 to 2.0 mM. (Other parameters remain constant including

DA=1.28 mg mL⁻¹, melamine concentration=2.56 mg mL⁻¹, pyrolysis at 800 °C. LSV curves measured in O₂-saturated 0.1 M HClO₄, scan rate: 10 mV s⁻¹, rotation rate: 1600 rpm).

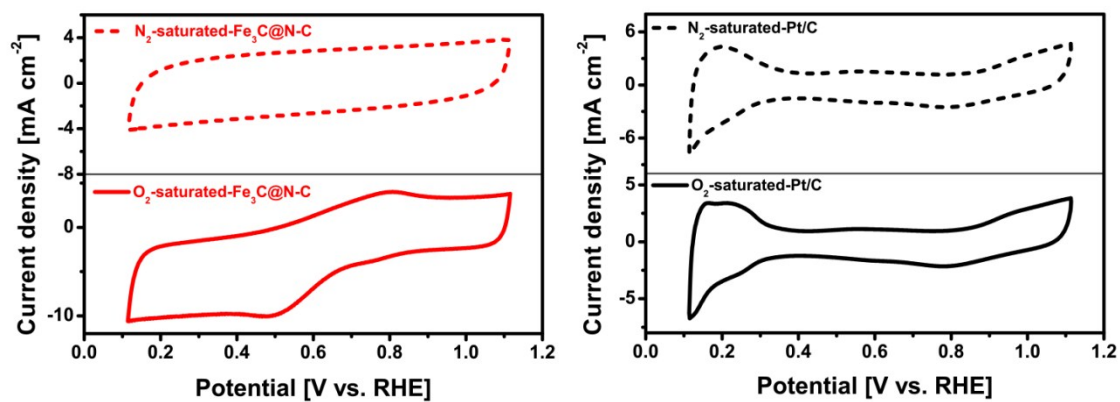


Fig. S15 CV curves of Fe₃C/N-C catalyst and Pt/C catalyst measured in O₂-saturated and N₂-saturated 0.1 M HClO₄, scan rate: 100 mV s⁻¹.

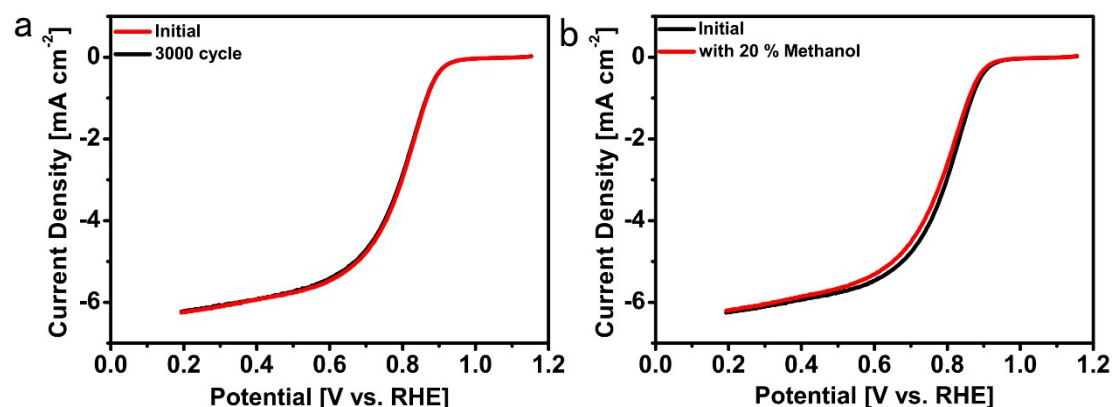


Fig. S16 (a) LSV curves of Fe/N-C catalyst before and after 3000-cycle ADT. (b) LSV curves with and without 20 % methanol (v/v). (Electrolytes: O₂-saturated 0.1 M HClO₄, scan rate: 10 mV s⁻¹, rotation rate: 1600 rpm).

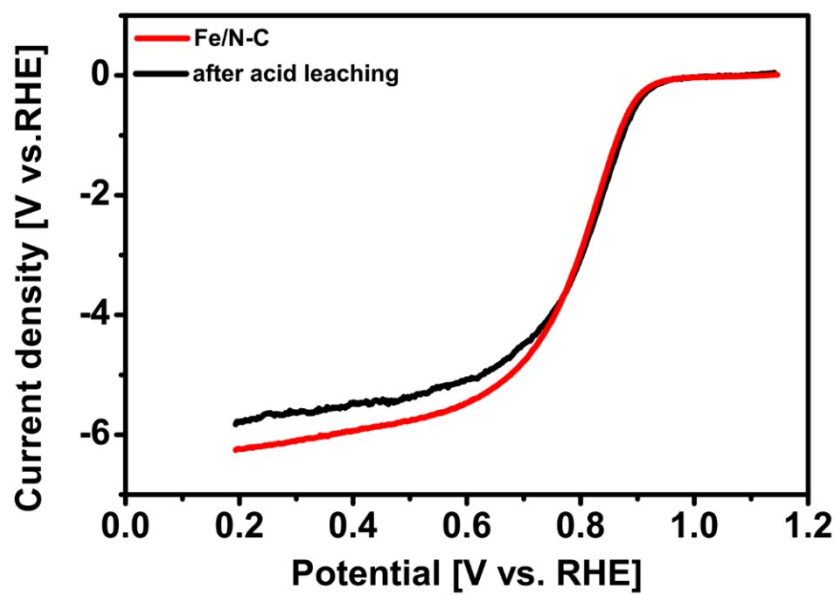


Fig. S17 (a) LSV curves of Fe/N-C catalyst before and after acid leaching and the second heat-treatment. (Electrolytes: O₂-saturated 0.1 M HClO₄, scan rate: 10 mV s⁻¹, rotation rate: 1600 rpm).

Table S1. ORR activity of Fe/N-C catalysts in alkaline media reported in recent literature.

Catalyst	Medium	$E_{1/2}$ (V vs. NHE)	$\Delta E_{1/2}$ (mV, relative to Pt/C)	n	Max H_2O_2 (%)	Ref.
Fe-N/C	0.1 M KOH	0.915	+45	3.81-3.99	5	This work
3D-Fe-N-CNS	0.1 M KOH	0.88	+20	3.83-3.95	-	[1]
Fe-ISAs/CN	0.1 M KOH	0.9	+58	3.9	5	[2]
Fe/SNC	0.1 M KOH	0.79	+40			[3]
Fe-N/C-800	0.1 M KOH	0.81	-	3.97	5	[4]
Fe SAC/N-C	0.1 M KOH	0.89	+40	4	2	[5]
SA-Fe-HPC	0.1 M KOH	0.89	+50	4	2.5	[6]
Fe-N-SCCF*	0.1 M KOH	0.883	-	3.9-4	5	[7]
Fe₅₀-N-C-900*	0.1 M KOH	0.92	+70	3.95	10	[8]
FeGH-ArNH3	0.1 M KOH	-	-27	3.95	5.6	[9]
Fe/N/C	0.1 M KOH	0.84	0	3.96	-	[10]
Fe SAs-N/C-20	0.1 M KOH	0.909	+59	3.8	-	[11]
Fe@Aza-PON	0.1 M KOH	-	+13	3.7	15	[12]
N-Fe-CNT/CNP	0.1M NaOH	0.93	+20	3.92	-	[13]
SA-Fe/NG	0.1 M KOH	0.88	+30	3.87-3.96	8.6	[14]
Fe@C-FeNCs	0.1 M KOH	0.899	+15	3.95-3.99	2.5	[15]
Fe-N/C-700*	0.1 M KOH	0.84	+5	4.02	3	[16]
Fe-N-CC	0.1 M KOH	0.83	+50	3.7	10	[17]
Fe_{SA}-N-C*	0.1 M KOH	0.891	+43	4	5.5	[18]
Fe-N-S*	0.1 M KOH	0.91	+60	4	2	[19]
Fe@NC-800*	0.1 M KOH	0.81	+40	3.98	3.55	[20]

Fe/Fe₃C@N-C*	0.1 M KOH	0.804	-16	4.08-4.15	3.5	[21]
Fe-N-C*	1 M NaOH	0.9	+20	3.9	-	[22]
Fe-N-C900*	0.1 M KOH	0.91	+32	3.988	2.5	[23]
CNT@f-FeNC170*	0.1 M KOH	0.84	0			[24]
SC-Fe*	0.1 M KOH	0.869	-	3.7	-	[25]
C-FeHZ8@g-C3N4-950*	0.1 M KOH	-	+30	3.96	-	[26]
Fe@N-CNTs@rGO *	0.1 M KOH	0.83	0	4.1	7	[27]

Table S2. ORR activity of Fe/N-C catalysts in acidic media reported in recent literature.

Catalyst	Medium	E_{1/2} (V vs. NHE)	ΔE_{1/2} (mV, relative to Pt/C)	n	Max H₂O₂ (%)	Ref.
Fe-N/C	0.1 M HClO ₄	0.810	-55	>3.95	2	This work
C-Fe-Z8-Ar*	0.1 M HClO ₄	0.82	-40	3.98	1	[28]
FeCo-NC	0.1 M HClO ₄	0.74	-	3.9	-	[29]
Fe-ISAs/CN	0.1 M HClO ₄	-	-90	-	-	[2]
Fe/SNC	0.5 M H ₂ SO ₄	0.77	-50	3.9	6	[3]
SA-Fe-HPC	0.1 M HClO ₄	0.81	-30	3.9	-	[6]
Fe-g-C3N4@C	0.1 M HClO ₄	0.75	-	3.95	2.6	[30]
Fe-NMCS	0.1 M HClO ₄	-	-59	3.92-3.94	6	[31]
Fe/N/S-PCNTs	0.5 M H ₂ SO ₄	0.62	-14	3.84	-	[32]
PmPDAFeNx/C	0.1 M H ₂ SO ₄	0.82	-65	-	1.5	[33]
(CM+PANI)-Fe-C	0.5 M H ₂ SO ₄	0.8	-	3.95	2.5	[11]
Fe/N/C-SCN	0.1 M H ₂ SO ₄	0.836	-48	-	1.5	[34]
Fe-N-C/VA-CNT	0.5 M H ₂ SO ₄	0.79	-	3.92-3.98	1-5	[35]

SA-Fe/NG	0.1 M HClO ₄	0.8	-30	3.95	5	[14]
Fe-N/C-700*	0.1 M HClO ₄	-	-18	3.98	5	[16]
Fe-N-CC*	0.5 M H ₂ SO ₄	0.56	-80	3.8	8	[17]
Fe _{SA} -N-C*	0.1 M HClO ₄	0.776	-5	4	1	[18]
Fe-N-S*	0.5 M H ₂ SO ₄	0.78	-15	4	1	[19]
Fe@NC-800*	0.5 M H ₂ SO ₄	0.58	-140	3.74	-	[20]
Fe-N-C900	0.5 M H ₂ SO ₄	0.80	-	3.955	2	[23]
CNT-Fe/NHCNS	0.1 M HClO ₄	0.84	+20	3.93-3.98	2	[36]
C-FeHZ8@g-C3N4-950*	0.1 M HClO ₄	-	-60	3.7	-	[26]

Reference

- [1] G. Wan, M. Ma, A. Jia, L. Chen, Y. Chen, X. Cui, H. Chen, J. Shi, *Journal of Materials Chemistry A* **2016**, *4*, 11625-11629.
- [2] Y. Chen, S. Ji, Y. Wang, J. Dong, W. Chen, Z. Li, R. Shen, L. Zheng, Z. Zhuang, D. Wang, Y. Li, *Angew Chem Int Ed Engl* **2017**, *56*, 6937-6941.
- [3] H. Shen, E. Gracia-Espino, J. Ma, K. Zang, J. Luo, L. Wang, S. Gao, X. Mamat, G. Hu, T. Wagberg, S. Guo, *Angew Chem Int Ed Engl* **2017**, *56*, 13800-13804.
- [4] W. Niu, L. Li, X. Liu, N. Wang, J. Liu, W. Zhou, Z. Tang, S. Chen, *J Am Chem Soc* **2015**, *137*, 5555-5562.
- [5] Y. Lin, P. Liu, E. Velasco, G. Yao, Z. Tian, L. Zhang, L. Chen, *Adv Mater* **2019**, *31*, e1808193.
- [6] Z. Zhang, J. Sun, F. Wang, L. Dai, *Angew Chem Int Ed Engl* **2018**, *57*, 9038-9043.
- [7] B. Wang, X. Wang, J. Zou, Y. Yan, S. Xie, G. Hu, Y. Li, A. Dong, *Nano Lett* **2017**, *17*, 2003-2009.
- [8] S. Fu, C. Zhu, D. Su, J. Song, S. Yao, S. Feng, M. H. Engelhard, D. Du, Y. Lin, *Small* **2018**, 1703118.
- [9] M. Wang, Y. Yang, X. Liu, Z. Pu, Z. Kou, P. Zhu, S. Mu, *Nanoscale* **2017**, *9*, 7641-7649.
- [10] Y. Yu, D. Xiao, J. Ma, C. Chen, K. Li, J. Ma, Y. Liao, L. Zheng, X. Zuo, *RSC Advances* **2018**, *8*, 24509-24516.
- [11] R. Jiang, L. Li, T. Sheng, G. Hu, Y. Chen, L. Wang, *Journal of the American Chemical Society* **2018**, *140*, 11594-11598.
- [12] S.-J. Kim, J. Mahmood, C. Kim, G.-F. Han, S.-W. Kim, S.-M. Jung, G. Zhu, J. J. De Yoreo, G. Kim, J.-B. Baek, *Journal of the American Chemical Society* **2018**, *140*, 1737-1742.

- [13] H. T. Chung, J. H. Won, P. Zelenay, *Nat Commun* **2013**, *4*, 1922.
- [14] L. Yang, C. D, X. H, Z. X, W. X, S. J, X. Z, C. D, *Proceedings of the National Academy of Sciences of the United States of America* **2018**, *115*, 6626.
- [15] W. J. Jiang, L. Gu, L. Li, Y. Zhang, X. Zhang, L. J. Zhang, J. Q. Wang, J. S. Hu, Z. Wei, L. J. Wan, *J Am Chem Soc* **2016**, *138*, 3570-3578.
- [16] Z. K. Yang, L. Lin, A. W. Xu, *Small* **2016**, *12*, 5710-5719.
- [17] G. A. Ferrero, K. Preuss, A. Marinovic, A. B. Jorge, N. Mansor, D. J. L. Brett, A. B. Fuertes, M. Sevilla, M.-M. Titirici, *ACS Nano* **2016**, *10*, 5922-5932.
- [18] L. Jiao, G. Wan, R. Zhang, H. Zhou, S. H. Yu, H. L. Jiang, *Angewandte Chemie International Edition* **2018**, *57*, 8525-8529.
- [19] H. Jin, H. Zhou, D. He, Z. Wang, Q. Wu, Q. Liang, S. Liu, S. Mu, *Applied Catalysis B: Environmental* **2019**, *250*, 143-149.
- [20] L. Zhang, C. Qi, A. Zhao, G. Xu, J. Xu, L. Zhang, C. Zhang, D. Jia, *Applied Surface Science* **2018**, *445*, 462-470.
- [21] C. Song, S. Wu, X. Shen, X. Miao, Z. Ji, A. Yuan, K. Xu, M. Liu, X. Xie, L. Kong, G. Zhu, S. Ali Shah, *J Colloid Interface Sci* **2018**, *524*, 93-101.
- [22]
- [23] D. Lyu, Y. B. Mollamahale, S. Huang, P. Zhu, X. Zhang, Y. Du, S. Wang, M. Qing, Z. Q. Tian, P. K. Shen, *Journal of Catalysis* **2018**, *368*, 279-290.
- [24] G. Zhang, Y. Jia, C. Zhang, X. Xiong, K. Sun, R. Chen, W. Chen, Y. Kuang, L. Zheng, H. Tang, W. Liu, J. Liu, X. Sun, W.-F. Lin, H. Dai, *Energy & Environmental Science* **2019**, *12*, 1317-1325.
- [25] J. Xie, B. Q. Li, H. J. Peng, Y. W. Song, J. X. Li, Z. W. Zhang, Q. Zhang, *Angew Chem Int Ed Engl* **2019**, *58*, 4963-4967.
- [26] Y. Deng, B. Chi, X. Tian, Z. Cui, E. Liu, Q. Jia, W. Fan, G. Wang, D. Dang, M. Li, K. Zang, J. Luo, Y. Hu, S. Liao, X. Sun, S. Mukerjee, *Journal of Materials Chemistry A* **2019**, *7*, 5020-5030.
- [27] X. Han, Z. Zheng, J. Chen, Y. Xue, H. Li, J. Zheng, Z. Xie, Q. Kuang, L. Zheng, *Nanoscale* **2019**.
- [28] X. Wang, H. Zhang, H. Lin, S. Gupta, C. Wang, Z. Tao, H. Fu, T. Wang, J. Zheng, G. Wu, X. Li, *Nano Energy* **2016**, *25*, 110-119.
- [29] Z. Zhang, M. Dou, H. Liu, L. Dai, F. Wang, *Small* **2016**, *12*, 4193-4199.
- [30] M.-Q. Wang, W.-H. Yang, H.-H. Wang, C. Chen, Z.-Y. Zhou, S.-G. Sun, *ACS Catalysis* **2014**, *4*, 3928-3936.
- [31] F. L. Meng, Z. L. Wang, H. X. Zhong, J. Wang, J. M. Yan, X. B. Zhang, *Adv Mater* **2016**, *28*, 7948-7955.
- [32] Z. Tan, H. Li, Q. Feng, L. Jiang, H. Pan, Z. Huang, Q. Zhou, H. Zhou, S. Ma, Y. Kuang, *Journal of Materials Chemistry A* **2019**, *7*, 1607-1615.
- [33] Q. Wang, Z.-Y. Zhou, Y.-J. Lai, Y. You, J.-G. Liu, X.-L. Wu, E. Terefe, C. Chen, L. Song, M. Rauf, N. Tian, S.-G. Sun, *Journal of the American Chemical Society* **2014**, *136*, 10882-10885.
- [34] W. Yu-Cheng, L. Yu-Jiao, S. Lin, Z. Zhi-You, L. Jian-Guo, W. Qiang, Y. Xiao-Dong, C. Chi, S. Wei, Z. Yan-Ping, *Angewandte Chemie* **2015**, *54*, 9907-9910.
- [35] S. Yasuda, A. Furuya, Y. Uchibori, J. Kim, K. Murakoshi, *Advanced Functional Materials* **2016**, *26*, 738-744.

[36] J.-C. Li, M. Cheng, T. Li, L. Ma, X. Ruan, D. Liu, H.-M. Cheng, C. Liu, D. Du, Z. Wei, Y. Lin, M. Shao, *Journal of Materials Chemistry A* **2019**, *7*, 14478-14482.